


Topically applied liposome-in-hydrogels for systematically targeted tumor photothermal therapy

Gang Chen^{a*}, Aftab Ullah^{b,c,*#}, Gang Xu^d, Zhou Xu^a, Fei Wang^a, Tianqing Liu^{b,e}, Yi Su^f, Tangjie Zhang^a and Kaikai Wang^b 

^aInstitute of Comparative Medicine, College of Veterinary Medicine, Jiangsu Co-innovation Center for Prevention and Control of Important Animal Infectious Diseases and Zoonoses, Joint International Research Laboratory of Agriculture and Agri-Product Safety, The Ministry of Education of China, Yangzhou University, Yangzhou, China; ^bSchool of Pharmacy, Nantong University, Nantong, China; ^cDepartment of Pharmacy, Shantou University Medical College, Shantou, China; ^dDepartment of Burn and Plastic Surgery, Clinical Medical College, Yangzhou University, Yangzhou, China; ^eNICM Health Research Institute, Western Sydney University, Westmead, Australia; ^fDepartment of Medical, Jinling Hospital, Medical School of Nanjing University, Nanjing, China

ABSTRACT

Transdermal drug delivery for local or systemic therapy provides a potential anticancer modality with a high patient compliance. However, the drug delivery efficiency across the skin is highly challenging due to the physiological barriers, which limit the desired therapeutic effects. In this study, we prepared liposome-in-hydrogels containing a tumor targeting photosensitizer IR780 (IR780/lipo/gels) for tumor photothermal therapy (PTT). The formulation effectively delivered IR780 to subcutaneous tumor and deep metastatic sites, while the hydrogels were applied on the skin overlying the tumor or on an area of distant normal skin. The photothermal antitumor activity of topically administered IR780/lipo/gels was evaluated following laser irradiation. We observed significant inhibition of the rate of the tumor growth without any toxicity associated with the topical administration of hydrogels. Collectively, the topical administration of IR780/lipo/gels represents a new noninvasive and safe strategy for targeted tumor PTT.

ARTICLE HISTORY

Received 20 July 2021
Revised 21 August 2021
Accepted 23 August 2021

KEYWORDS






IR780; liposome-in-hydrogels; transdermal drug delivery; photothermal therapy; topical application

1. Introduction

The human skin, covering a large surface area of approximately 2 m², is considered to be a potential region for drug delivery (Kilian et al., 2015). In comparison with other drug administration routes, the transdermal drug delivery for topical applications is preferred due to convenient self-administration, suitability for long-term treatment, avoidance of the first-pass effect, and improved patient compliance (Jiang et al., 2018). Topical drug administration through the skin provides an effective strategy with high therapeutic concentration and minimized systemic toxicity to deliver drugs for local or systemic therapy (Jiang et al., 2018). However, delivery of drugs across the skin barrier is highly challenging. Stratum corneum, the outermost layer of the skin, is the most significant barrier to transdermal drug delivery (Menon et al., 2012). It serves as a brick and mortar system consisting of layers of flattened dead keratinocytes surrounded by a lipid matrix. Currently, several mechanical devices have been used to improve the transdermal efficiency of drugs by physical


enhancement techniques such as electroporation (Prausnitz, 1999), iontophoresis (Wang et al., 2005), magnetophoresis (Murthy et al., 2010), sonophoresis (Azagury et al., 2014), and microneedle (Prausnitz, 2004; Lee et al., 2016a). Alternatively, nanoparticle-based drug delivery systems have been increasingly exploited for transdermal drug delivery (Neubert, 2011; Roberts et al., 2017), such as liposomes (Seong et al., 2018), nanoemulsions (Rai et al., 2018), dendritic nanocarriers (Yang et al., 2014), and inorganic nanosystems (Siu et al., 2014; Lee et al., 2016b). Often phospholipid-based liposomes are biocompatible and easy to formulate, and have the remarkable ability to encapsulate both hydrophobic and hydrophilic compounds (Pitorre et al., 2017). Interestingly, liposomal formulations can penetrate the stratum corneum barrier, resulting in the drug delivery close to the lesion and thus enhancing the delivery of loaded drugs (Fadel et al., 2009; Conde et al., 2016; Pitorre et al., 2017; Wu et al., 2021).

Meanwhile, nanoparticles are increasingly combined with other biomaterials to form hybrid nanostructures for improved therapeutic index. Recently, hydrogels with

CONTACT Kaikai Wang  kirk2008@126.com  School of Pharmacy, Nantong University, Nantong 226001, China; Yi Su  939596868@qq.com  Department of Medical, Jinling Hospital, Medical School of Nanjing University, Nanjing, Jiangsu 210002, China; Tangjie Zhang  slx@yzu.edu.cn Institute of Comparative Medicine, College of Veterinary Medicine, Jiangsu Co-innovation Center for Prevention and Control of Important Animal Infectious Diseases and Zoonoses, Joint International Research Laboratory of Agriculture and Agri-Product Safety, The Ministry of Education of China, Yangzhou University, Yangzhou 225009, China

*Both authors contributed equally to this work.

#Department of cerebrovascular diseases, the second hospital of Zhengzhou University, Zhengzhou, China.

 Supplemental data for this article can be accessed [here](#).

© 2021 The Author(s). Published by Informa UK Limited, trading as Taylor & Francis Group.

This is an Open Access article distributed under the terms of the Creative Commons Attribution-NonCommercial License (<http://creativecommons.org/licenses/by-nc/4.0/>), which permits unrestricted non-commercial use, distribution, and reproduction in any medium, provided the original work is properly cited.

hydrophilic 3D polymer networks have gained considerable attention for biomedical applications including tissue engineering and drug delivery systems due to their unique characteristics (e.g. high water content and hydrophilicity) (Wichterle & Lím, 1960; Hamidi et al., 2008; Appel et al., 2015; Choe et al., 2018). Hydrogel can be loaded with nanoparticles such as liposomes for loco-regional targeting of superficial tumors (Mulik et al., 2009; Bai et al., 2018). This targeted delivery strategy can boost the efficacy of loaded therapeutic agents penetrating into the tumor tissue in high concentrations (Matai et al., 2020). With appropriate compositions, hydrogels can not only preserve the structural integrity and the functionalities of the contained nanoparticles, but also offer additional engineered flexibility to improve the therapeutic efficacy (Appel et al., 2015). The adhesive nanoparticle-loaded hydrogel patch enhanced the stability of doped nanoparticles and provided the local and systemic delivery of embedded nanoparticles (Conde et al., 2016).

Near infrared light (NIR)-mediated photothermal therapy (PTT) has become an attractive tumor treatment method and alternative to traditional cancer treatment (Doughty et al., 2019; Su et al., 2019). Photo-responsive nanomaterials which absorb light in the NIR window (700–1100 nm) can generate heat to induce hyperthermia in the tumor tissues and simultaneously cause irreversible cellular damage, leading to tumor eradication (Li et al., 2019; Yu et al., 2019). Compared with the clinically used photosensitizer, such as ICG, IR780 is more stable and has higher fluorescence intensity (Zhang et al., 2010). In addition, as a recently developed photosensitizer, IR780 is a lipophilic organic dye that absorbs NIR light and exhibits excellent photothermal effects. As a lipophilic cation, IR780 can accumulate in a broad range of tumors without additional chemical conjugation to achieve tumor targeting, which is attributed to the higher negative inside transmembrane potentials of mitochondria in tumor cells than normal cells (Davis et al., 1985; Zhang et al., 2010, 2014). Therefore, IR780 has a great potential for tumor targeting and anticancer ability (Yue et al., 2013; Zhang et al., 2014; Guo et al., 2015). To the best of our knowledge, IR780 formulations were developed for oral, intravenous (i.v.), or intraperitoneal (i.p.) administration in most currently published reports (Chen et al., 2016).

Inspired by the numerous advantages of hydrogels in retaining nanoparticles and enhancing their physicochemical properties, herein, we report an advanced liposome-in-hydrogel hybrid system for systematic delivery of photosensitizers via topical administration. We hypothesize that the targeted tumor PTT will be achieved by encapsulation of IR780 into liposomes and then incorporated the liposomes in hydrogels for the treatment of cancer. Such formulation judiciously integrates two distinct materials into one robust hybrid system with unique physicochemical and biological properties that either one of the two building blocks cannot achieve independently.

2. Materials and methods

2.1. Materials

IR780 iodide and IR792 perchlorate were purchased from Sigma-Aldrich (St. Louis, MO). Cholesterol and egg

phosphatidylcholine were obtained from Aladdin Industrial Corporation (Shanghai, China). Poloxamer 407 (P407) and Poloxamer 188 (P188) were purchased from Sigma-Aldrich (St. Louis, MO). Mouse colon cancer cell line (CT-26) and mouse breast cancer cell line (4T1) were purchased from Shanghai Institute of Cell Biology (Shanghai, China). Unless otherwise stated, all other reagents were from Nanjing Well Offer Biotechnology Co., Ltd. (Nanjing, China).

2.2. Preparation of IR780-in-liposome-in-hydrogels

Liposomes were prepared by the thin-film hydration method. Briefly, phosphatidylcholine, cholesterol, and IR780 were dissolved in dichloromethane. The mass ratios of phosphatidylcholine, cholesterol, and IR780 were 175:75:3. The organic solvent was removed by rotary evaporation at 30 °C and obtained dried thin film. Then, the lipid film was hydrated with PBS aqueous solution for 30 min. The unincorporated IR780 was removed by ultrafiltration (molecular weight cutoff (MWCO)=10 kDa) at 12,000 rpm at 4 °C for 30 min.

Hydrogels were prepared by the cold process (Soga et al., 2005). P407 (1.25 g) was added into 5 mL of cold liposome solutions and left overnight at 4 °C to complete dissolve the polymers. Then, P188 (0.25 g) were added and placed at 4 °C for 4–6 h to allow the gelation to occur.

2.3. Physical characterization of liposomes and hydrogels

The hydrodynamic size of the prepared liposomes was assessed by Zeta Plus. The morphology of liposomes and hydrogels was measured by TEM and SEM. The absorption spectra of free IR780, IR780 liposomes (IR780/lipo), and IR780-in-liposome-in-hydrogels (IR780/lipo/gel) were recorded using UV-vis spectrophotometer to calculate IR780 content in liposomes or hydrogels. The rheological analysis of the hydrogel samples was carried out at 37 °C. The strain was kept at 0.1% and a dynamic frequency sweep from 0.1 to 10 rad/s was conducted to measure the storage modulus G' and loss modulus G'' .

IR780/lipo/gels were incubated in release medium (pH 7.4 PBS) at 37 °C. At desirable time intervals, supernatant was withdrawn and measured the particle size of the liposomes released from the hydrogel using dynamic light scattering (DLS). To investigate the amount of IR780 loaded liposomes released from the hydrogels, the IR780 content was detected using UV-Vis spectrophotometer.

2.4. Establishment of subcutaneous tumor model and lung metastasis model

All animal experiments were conducted in compliance with the Animal Care and Use Committee of Yangzhou University. Pathogen-free five-week-old Balb/c male mice were used to establish allograft tumor model. Briefly, 0.2 mL of PBS contained 1×10^7 CT-26 cells was injected into the normal mice. When the volume of tumors reached about 200 mm³ after two weeks, the tumors were dissected and cut into about

1 mm³ pieces. In order to establish subcutaneous tumors for the biodistribution and therapeutic studies, the pieces of tumors (one each mouse) were injected into the flank region of the mice subcutaneously. When the volume of average tumor size reaches 200 mm³, the mice were used in subsequent experiments.

For the lung metastasis model, 5×10^5 4T1 cells were i.v. injected into pathogen-free five-week-old Balb/c male via the tail vein. On day 11, the mice were used in subsequent experiments.

2.5. Biodistribution of photosensitizers in subcutaneous tumor model and lung metastasis model

To evaluate the distribution of IR780 in primary tumor, the CT-26 tumor-bearing mice were randomly divided into six groups ($n = 3$). IR780/lipo/gel was patched onto the skin of tumor and back of mice to compare the topical or systematic delivery of photosensitizers (1.0 mg/kg photosensitizer). In addition to the transdermal drug delivery, IR780/lipo was i.v. injected via the tail vein to compare the route of drug delivery (dose of IR780 around 0.3 mg/kg). IR792 was used as a nontarget photosensitizer to illustrate the effects of tumor accumulation in comparison with IR780 (Lai et al., 2019). IVIS Lumina imaging system (Xenogen Co., Hopkinton, MA) was used to detect the fluorescent signal of photosensitizers for *in vivo* biodistribution study at 12–96 h. The amount of IR780 or IR792 in tissues was analyzed by IVIS Living imaging software. The tumors were sectioned and stained with Hoechst to detect IR780 fluorescence in the tumors (Wuhan Servicebio Technology, Wuhan, China).

To evaluate the distribution of IR780 in metastasis, a lung metastasis model was established as described above ($n = 3$). IR780/lipo/gel and IR792/lipo/gel were patched onto the skin of back of mice (1.0 mg/kg photosensitizer). IR780/lipo and IR792/lipo were i.v. injected via the tail vein. In addition, the normal mice were patched onto the skin of back as a control. *In vivo* fluorescence images were recorded at 48 h after administration.

2.6. Anticancer activity in tumor-bearing mice

When the volume of average tumor size reaches 200 mm³, the mice were randomly divided into five groups ($n = 6$), which were treated with PBS (on the skin of tumor), IR780/lipo/gel (on the skin of back) plus NIR laser irradiation, IR780/lipo/gel (on the skin of tumor) plus NIR laser irradiation, IR792/lipo/gel (on the skin of back) plus NIR laser irradiation, and IR792/lipo/gel (on the skin of tumor) plus NIR laser irradiation, respectively. The dosage of IR780 or IR792 was 7 mg/kg. The day of administration was designated as day 0. After 48 h, NIR laser irradiation (2 W/cm², 1 min) was used to irradiate the tumors. Treatment administration and laser irradiation were repeated on days 3 and 5, respectively. The administration was performed under dark condition. Body weights and tumor sizes were recorded every other day after laser treatment. Tumor volume (V) was calculated according to the following formula: $\text{width}^2 \times \text{length} / 2$, where length is

the longest diameter of the tumor, width is the shortest, respectively. On day 16, all of the mice were sacrificed, and all the tumor tissues were collected for further analysis.

2.7. Safety of liposome-in-hydrogels

To evaluate the skin toxicity of drug delivery system, mice were shaved on the back 24 h prior to the study. Then, the IR780/lipo/gel was applied on the shaved area once daily for a period of seven days. At the end of the experiment, the mice were sacrificed, and the skin was sectioned for hematoxylin and eosin (H&E) staining. Serum levels of alanine aminotransferase (ALT), aspartate transaminase (AST), and blood urea nitrogen (BUN) were analyzed by Wuhan Servicebio Technology (Wuhan, China).

2.8. Statistical analysis

Statistical assessments were conducted using a two-sided Student's *t*-test for two groups ($p < .05$ was considered statistically significant). * $p < .05$, ** $p < .01$, *** $p < .005$, vs. the relevant group as illustrated in the figure legends. The results are shown as the means \pm SD.

3. Results and discussion

3.1. Preparation and characterization of IR780/lipo/gels

The composition of liposome in hydrogel formulation is illustrated in Figure 1(A). The preparation of IR780/lipo/gels can be divided into two steps. In the first step, we prepared IR780/lipo following a previously established protocol (Matai et al., 2020). The particle size of the liposomes was around 130 nm with polydispersity of 0.185 determined by DLS (Figure 1(B)). The TEM image showed that the IR780/lipo was relatively spherical in shape as shown in Figure 1(C). The IR780 content in the liposomes was 0.9 wt% determined by UV–vis spectrophotometer. In addition, IR792 was used as a nontarget photosensitizer to prepare liposomes. As shown in Figure S1, the particle size (122 nm) and morphology (spherical nanoparticles) of the IR792/lipo were similar with IR780/lipo. In the second step, we prepared hydrogels using the cold method (Schmolka, 1972). The morphological observation showed that the freeze dried IR780/lipo/gels were characteristic porous sponge-like structures (Figure 1(D)). The rheological properties of the hydrogels were characterized with measurements of the storage modulus (G') and the loss modulus (G''). As shown in Figure 1(E), G' exceeded G'' over the entire frequency range, a clear viscoelastic behavior indicating the formation of a hydrogel network. The absorption spectra of IR780 in liposomes and hydrogels were evaluated using UV–vis spectroscopy (Figure 1(F)). As anticipated, the IR780/lipo and IR780/lipo/gel showed similar absorption peaks with free IR780 in DMSO, which confirmed successful loading of the dye. Next, we investigated the release kinetics of liposomes from the hydrogels. The amount of released liposomes was quantified by measuring the amount of IR780 encapsulated in liposomes. Overall, the liposomes were

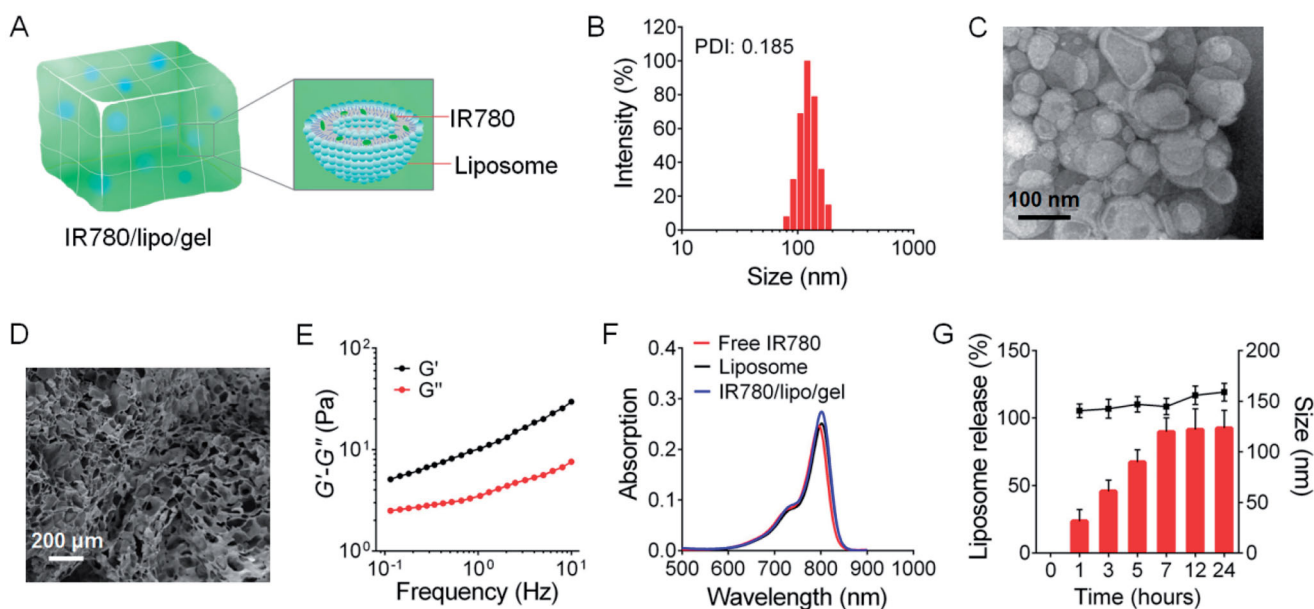


Figure 1. Preparation and characterization of IR780-in-liposome-in-hydrogels (IR780/lipo/gel). (A) Schematic illustration of IR780/lipo/gel. (B) Hydrodynamic size (diameter, nm) and PDI of IR780 liposomes (IR780/lipo). (C) Representative TEM images of IR780/lipo (scale bar: 100 nm). (D) Representative SEM images of IR780/lipo/gel (scale bar: 200 μm). (E) Rheological characterization of IR780/lipo/gel. The storage modulus G' and loss modulus G'' were plotted logarithmically against frequency (0.1–10 Hz at 37 $^{\circ}\text{C}$). (F) Absorption spectra of free IR780, IR780/lipo, and IR780/lipo/gel. (G) *In vitro* release of liposomes from the hydrogel. Data are presented as the means \pm SD ($n = 3$).

released in a time dependent order. Specifically, more than 90% liposomes were released at 12 h (Figure 1(G)). In addition, the particle sizes showed that the liposomes remained stable after release from the hydrogel.

3.2. *In vivo* tracking of photosensitizers in CT-26 tumor-bearing mice

To evaluate the feasibility of topical administration of hydrogels for tumor imaging and antitumor PTT, a whole animal NIR imaging approach was conducted in CT-26 tumor-bearing mice. IR792/lipo and IR792/lipo/gel were prepared as controls to confirm the tumor targeting of IR780. IR780/lipo and IR792/lipo were administered by i.v. injection (0.3 mg/kg photosensitizer) and the hydrogels were applied topically on the skin of tumor or back (1.0 mg/kg photosensitizer). *In vivo* fluorescence images were recorded at 12 h, 24 h, 48 h, and 96 h after administration. After i.v. injection, the fluorescence intensity of IR780 was distributed throughout the whole body, while IR780 was accumulated specifically in the tumor region at 48 h exhibiting the tumor-targeted behavior of IR780. However, in the case of IR792, no tumor-specific accumulation was observed, suggesting only IR780 is the tumor-targeting agent (Figure 2(A)). Next, IR780/lipo/gel or IR792/lipo/gel was applied either on the skin overlying the tumor or on an area of normal skin (back). As shown in Figure 2(B,C), IR780 showed a significant accumulation in tumor at 48 h no matter where the hydrogel patched. After that, the fluorescence intensity of both dyes decreased over time. In summary, compared to IR792, the i.v. or topical administration of IR780 exhibited the highest tumor accumulation, beyond the restriction of patching site (Figure 2(D)).

In addition, the major organs and tumors were harvested at 72 h post administration and imaged *ex vivo*. As shown in

Figure 3(A,B), compared to the major organs, IR780 was mostly retained in the tumors and displayed highest fluorescence intensity suggesting maximum systemic absorption of the dye and tumor targeting. In contrast, the mice administered IR792/lipo or IR792/lipo/gel showed very weak systemic absorption and low accumulation of IR792 in the distant tumor except the topical application on the tumor. Quantification of the fluorescence signals in the tumors and other tissues further confirmed increased bioavailability of IR780 when given as patch (Figure 3(B)). Furthermore, compared to IR792/lipo/gel, a strong IR780 fluorescence (red) was also observed in tumor tissue sections of mice treated with patch on the back (Figure 3(C)). These findings revealed that the IR780/lipo/gel possessed the ability of systematic targeting to tumors after topical administration.

3.3. *In vivo* fluorescence biodistribution of photosensitizers in lung metastatic mice

To evaluate the targeting capability of IR780/lipo/gel to deep metastases, the *in vivo* distribution was evaluated in a lung metastatic mice model after i.v. injection of IR780/lipo or IR792/lipo, and topically application of IR780/lipo/gel or IR792/lipo/gel onto the back of mice. 4T1 cells, one of the most aggressive metastatic mouse breast cancer cell lines, were used to develop the metastatic breast cancer model [29–32]. The captured images showed that the negligible fluorescence signals were present in the whole body and *ex vivo* lungs of normal mice in both IR792/lipo/gel and IR780/lipo/gel groups (Figure 4(A,B)). However, compared to IR792/lipo, the fluorescence intensity in the metastases was significantly increased in the IR780/lipo treatment group, suggesting the tumor targeting behavior of IR780. Moreover, upon topical application of IR780/lipo/gel, the fluorescence signals

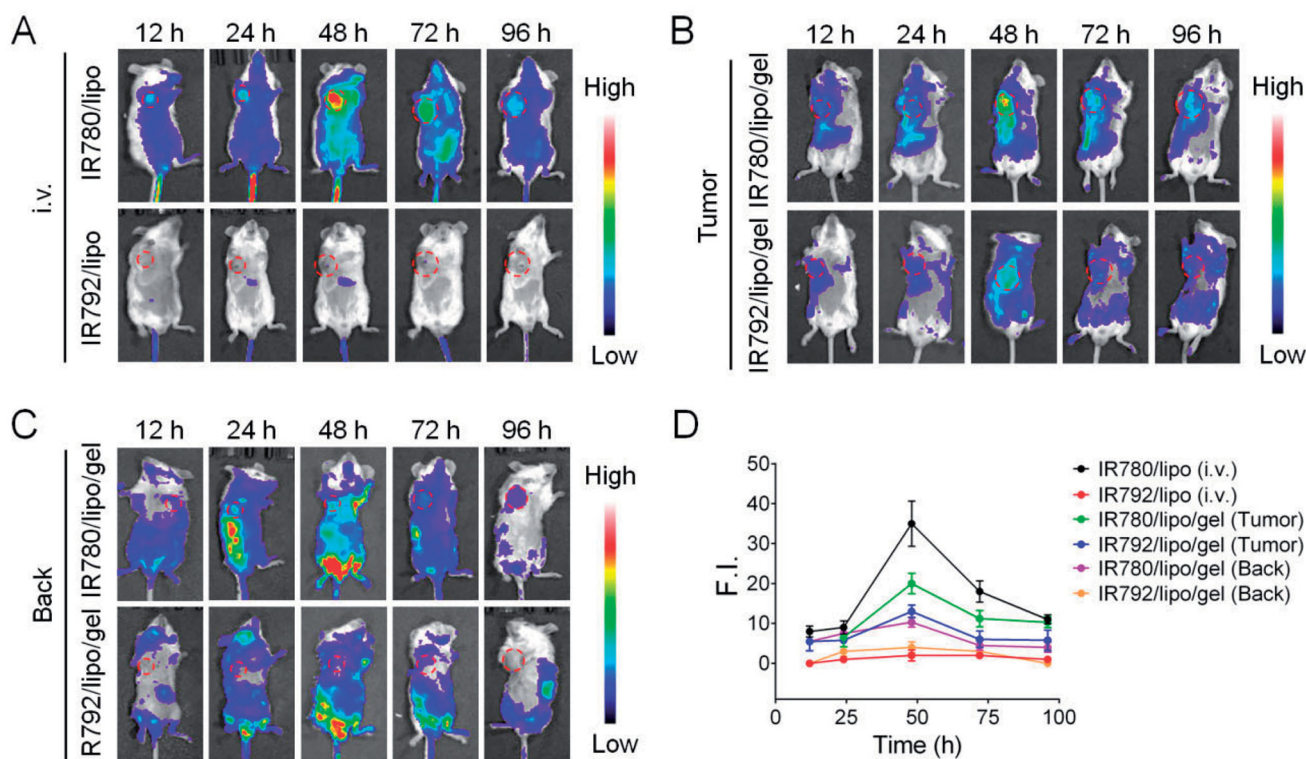


Figure 2. *In vivo* fluorescence imaging and biodistribution of photosensitizers in CT-26 tumor-bearing mice. (A) *In vivo* dye fluorescence images in CT-26 tumor-bearing mice at different time after intravenous injection (i.v.) of IR780/lipo and IR792/lipo. *In vivo* dye fluorescence images in CT-26 tumor-bearing mice after topically application of IR780/lipo/gel and IR792/lipo/gel onto the tumor (B) and the back (C) of mice. (D) F.I. of IR780 and IR792 in the tumors. Data are presented as the means \pm SD ($n = 3$).

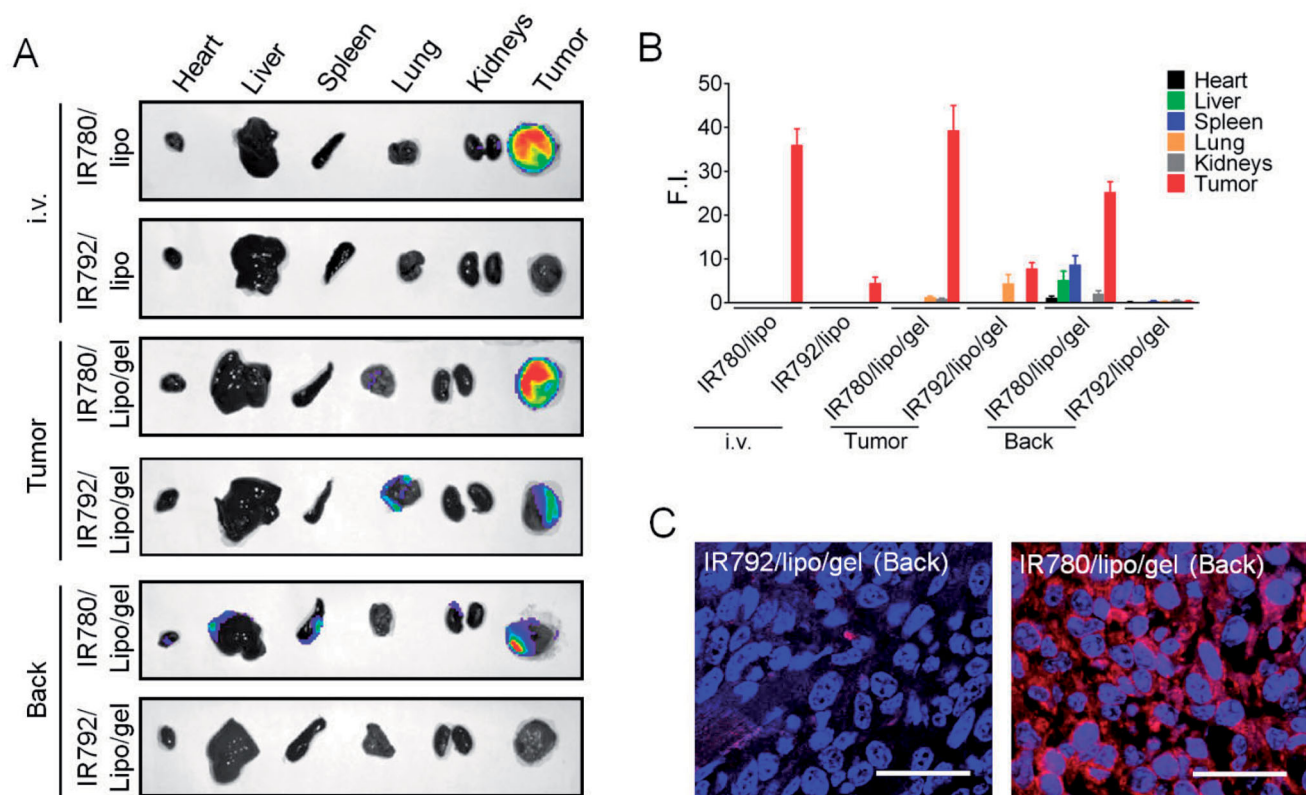


Figure 3. Organ distribution of dye. (A) Representative *ex vivo* fluorescence images of major organs and tumors after i.v. and topically application of IR780/lipo/gel and IR792/lipo/gel onto the tumor and the back of mice at 72 h. (B) F.I. of IR780 and IR792 in the major organs and tumors. (C) IR792 and IR780 fluorescence imaging in tumor sections following topically application of IR792/lipo/gel and IR780/lipo/gel onto the back. Data are presented as the means \pm SD ($n = 3$).

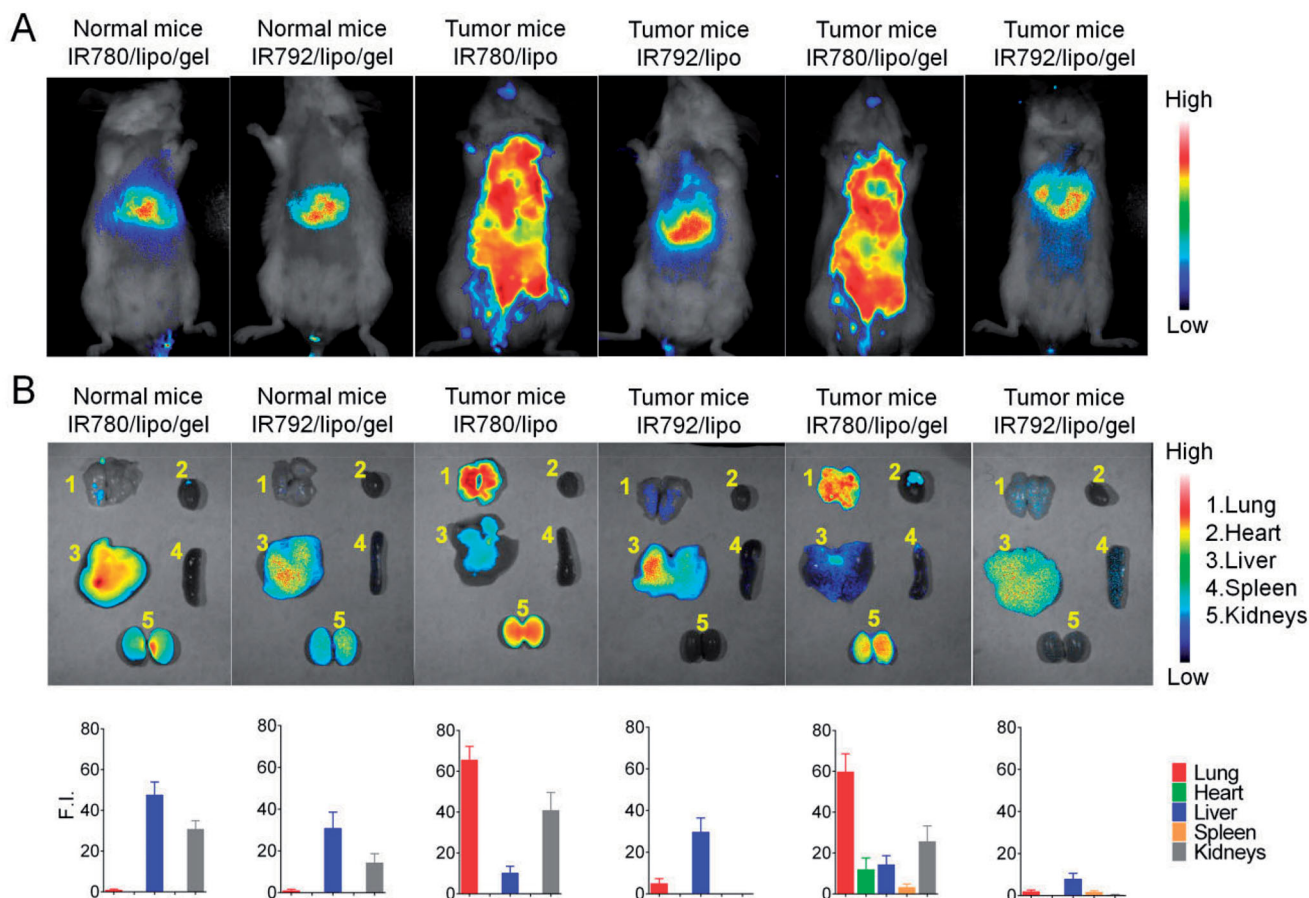


Figure 4. *In vivo* fluorescence imaging and biodistribution of photosensitizers in experimental lung metastasis model. (A) *In vivo* dye fluorescence images in experimental lung metastasis model or normal mice at 48 h after i.v. of IR780/lipo, IR792/lipo and topical application of IR780/lipo/gel and IR792/lipo/gel onto the back of mice. (B) Representative *ex vivo* fluorescence images and F.I. of IR780 and IR792 of major organs and tumors from the mice in (A). Data are presented as the means \pm SD ($n = 3$).

were specifically increased in the lung, thus further confirming the excellent targeting ability of IR780 to the deep metastases by topical application. Quantification of the fluorescence confirmed the whole body and *ex vivo* imaging results (Figure 4(B)).

3.4. Anticancer effect of the photothermal treatment with liposome-in-hydrogels

We then evaluated anticancer effects of the liposome-in-hydrogels upon NIR laser irradiation in CT-26 colon cancer mouse model. As shown in Figure 5(A), the tumors of the mice treated with PBS and IR792/lipo/gel (back) showed rapid tumor growth. Compared to the IR792/lipo/gel applied on the back, the IR792/lipo/gel group applied topically to the tumor showed decreased tumor size, possibly attributed to the comparatively more photosensitizer accumulation at the tumor site ($p < .01$). However, the topically applied IR780/lipo/gel exhibited maximum therapeutic effects showing targeted IR780 accumulation regardless of application onto the back or tumor ($p < .01$). After animal sacrifice, the tumors were excised and imaged (Figure 5(B)). The tumors in the IR792/lipo/gel (tumor) and IR780/lipo/gel (back or tumor) groups were significantly smaller than the other treatments. Furthermore, the changes in body weight in all groups were

recorded to assess the physiological toxicity of the different formulations. The tumor-bearing mice showed no significant body weight loss after topical administration of the liposome-in-hydrogels (Figure 5(C)). These results indicated that IR780/lipo/gel had systemic PTT efficacy after topical patching.

3.5. Safety of IR780-in-liposome-in-hydrogels

Finally, we evaluated the biosafety of the IR780/lipo/gels using a mouse skin model. In this study, the mouse back skin was shaved 24 h prior to gel application to allow the skin to recover from any possible disturbance to the stratum corneum. Then, the hydrogel samples were topically applied onto the skin. After a seven-days treatment, mouse skin treated with IR780/lipo/gel maintained its normal structure without any indications of toxicity such as erythema and edema, which was similar with the group treated with PBS (Figure 6(A)). Following the skin morphology examination, a skin biopsy was collected and stained with H&E. The IR780/lipo/gel treated skin maintained normal architecture, a clear layer of healthy epidermal cells on top of the dermis layer, which was identical to the PBS treated skin sample (Figure 6(B)). The absence of any skin reaction or toxicity within the seven-day treatment suggested that topical application of

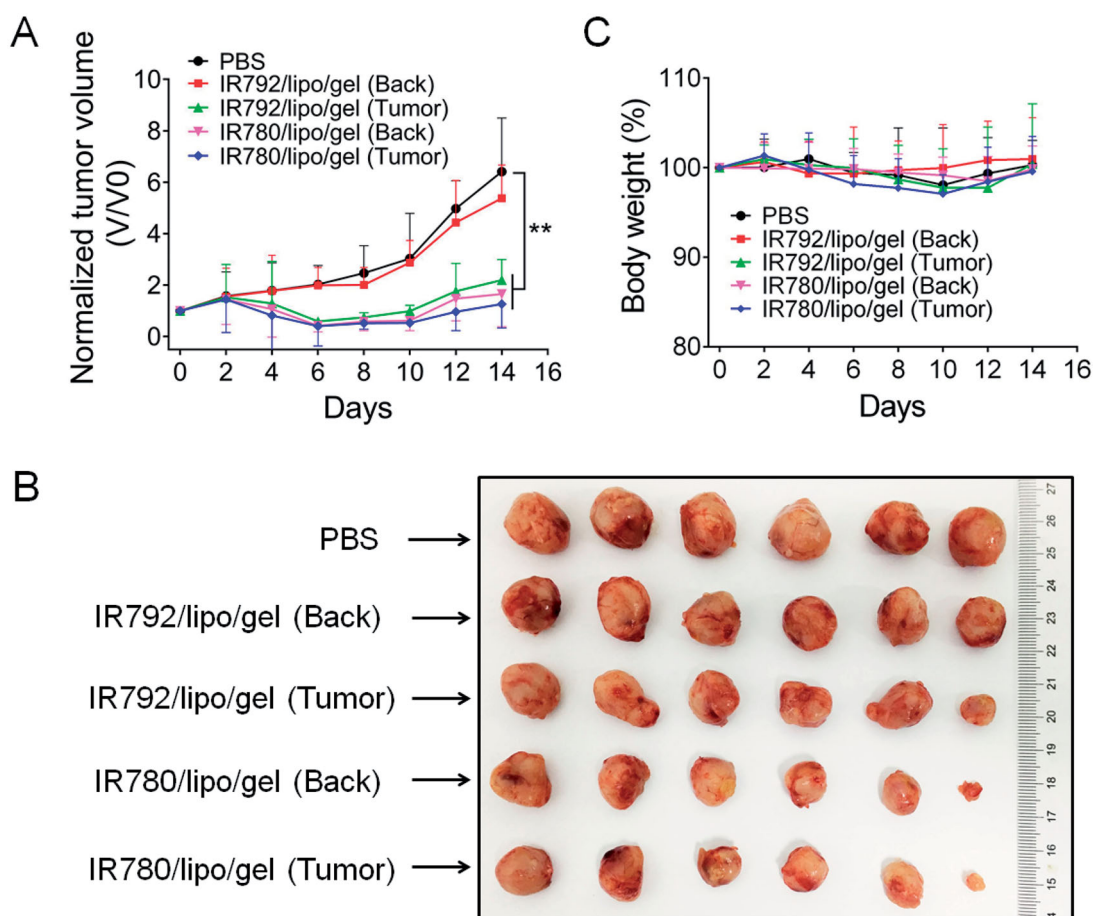


Figure 5. Photothermal anticancer therapy. (A) Antitumor PTT activity of IR780/lipo/gel and IR792/lipo/gel following topical application onto the back of mice in CT-26 colon cancer model. Outliers were removed to improve accuracy of the statistical results. (B) Images of excised tumors on day 14 after treatment. (C) Body weight changes over the treatment period. Data are presented as the means \pm SD ($n=6$). $**p < .01$, vs. the indicated groups.

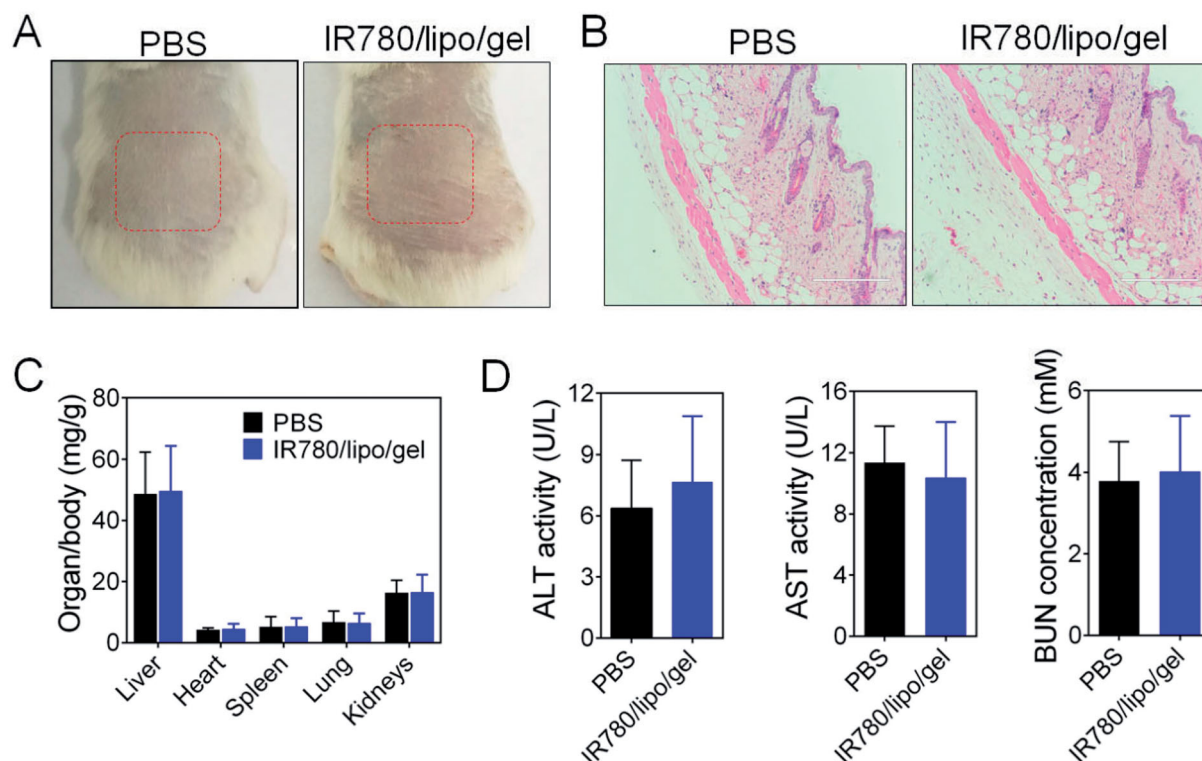


Figure 6. Safety of IR780/lipo/gel. (A) Skin morphology after topical application of IR780/lipo/gel. (B) The skin sections were further examined after H&E staining. (C) Weight ratios of organs to the total body weight and (D) quantification of ALT, AST, and BUN in the plasma after treatment with IR780/lipo/gel.

IR780/lipo/gel was safe for the skin. Next, major organs, including the heart, liver, spleen, and kidney and lungs, were then collected and weighted (Figure 6(C)). The organ/body weight changes in the IR780/lipo/gel group were similar to that in the PBS treated group. The main liver and kidney function markers including ALT, AST, and BUN were measured and no significant differences in any of the biomarker levels were observed between IR780/lipo/gel and PBS groups (Figure 6(D)). Overall, these findings suggest that the PTT with IR780/lipo/gel has excellent biocompatibility for cancer treatment.

4. Conclusions

In this study, we successfully developed a new photothermal therapeutic platform based on topical administered IR780/lipo/gels for systematical tumor therapy. Using subcutaneous tumor and lung metastatic models, we showed that this prepared hydrogel formulation effectively delivered IR780 to the tumor and lung metastasis. In addition, IR780/lipo/gel-treated mice showed excellent antitumor activity under laser irradiation, without producing any appreciable off-target toxicity. These results support the potential of IR780/lipo/gel as a safe theranostic platform for targeted PTT by topical administration. The reported formulation represents a noninvasive method of delivery that may further enhance the potential of PTT in human medicine. Taken together, integrating IR780 and liposomes with hydrogel technology provides a robust hybrid formulation for topical drug delivery against distant tumors.

Disclosure statement

No potential conflict of interest was reported by the author(s).

Funding

This work was supported by the National Natural Science Foundation of China [Grant Nos.: 31900993, 81903556], the General and Special Financial Grant from the China Postdoctoral Science Foundation [Grant No.: 2019M661956 and 2020T130561], the Postdoctoral Science Foundation Funded Project of Jiangsu Province [Grant No.: 2019K066], the Open Project Program of MOE Key Laboratory of Drug Quality Control and Pharmacovigilance [Grant No.: DQCP20/21PQ08], the Start-up Fund Provided by Yangzhou University [Grant No.: 5020/137011461], the Priority Academic Program Development of Jiangsu Higher Education Institutions (PAPD), and the Postdoc Fund by Shantou University Medical College, Shantou, Guangdong Province.

ORCID

Kaikai Wang  <http://orcid.org/0000-0002-1838-4394>

References

- Appel EA, Tibbitt MW, Webber MJ, et al. (2015). Self-assembled hydrogels utilizing polymer-nanoparticle interactions. *Nat Commun* 6:6295.
- Azagury A, Khoury L, Enden G, et al. (2014). Ultrasound mediated transdermal drug delivery. *Adv Drug Deliv Rev* 72:127–43.

- Bai R, Deng X, Wu Q, et al. (2018). Liposome-loaded thermo-sensitive hydrogel for stabilization of SN-38 via intratumoral injection: optimization, characterization, and antitumor activity. *Pharm Dev Technol* 23:106–15.
- Chen G, Wang K, Zhou Y, et al. (2016). Oral nanostructured lipid carriers loaded with near-infrared dye for image-guided photothermal therapy. *ACS Appl Mater Interfaces* 8:25087–95.
- Choe A, Yeom J, Shanker R, et al. (2018). Stretchable and wearable colorimetric patches based on thermoresponsive plasmonic microgels embedded in a hydrogel film. *NPG Asia Mater* 10:912–22.
- Conde J, Oliva N, Zhang Y, et al. (2016). Local triple-combination therapy results in tumour regression and prevents recurrence in a colon cancer model. *Nat Mater* 15:1128–38.
- Davis S, Weiss MJ, Wong JR, et al. (1985). Mitochondrial and plasma membrane potentials cause unusual accumulation and retention of rhodamine 123 by human breast adenocarcinoma-derived MCF-7 cells. *J Biol Chem* 260:13844–50.
- Doughty ACV, Hoover AR, Layton E, et al. (2019). Nanomaterial applications in photothermal therapy for cancer. *Materials* 12:779.
- Fadel M, Salah M, Samy N, et al. (2009). Liposomal methylene blue hydrogel for selective photodynamic therapy of acne vulgaris. *J Drugs Dermatol* 8:983–90.
- Guo F, Yu M, Wang J, et al. (2015). Smart IR780 theranostic nanocarrier for tumor-specific therapy: hyperthermia-mediated bubble-generating and folate-targeted liposomes. *ACS Appl Mater Interfaces* 7:20556–67.
- Hamidi M, Azadi A, Rafiei P. (2008). Hydrogel nanoparticles in drug delivery. *Adv Drug Deliv Rev* 60:1638–49.
- Jiang T, Wang T, Li T, et al. (2018). Enhanced transdermal drug delivery by transfersome-embedded oligopeptide hydrogel for topical chemotherapy of melanoma. *ACS Nano* 12:9693–701.
- Kilian D, Shahzad Y, Fox L, et al. (2015). Vesicular carriers for skin drug delivery: the Pheroid™ technology. *Curr Pharm Des* 21:2758–70.
- Lai J, Deng G, Sun Z, et al. (2019). Scaffolds biomimicking macrophages for a glioblastoma NIR-Ib imaging guided photothermal therapeutic strategy by crossing blood–brain barrier. *Biomaterials* 211:48–56.
- Lee H, Choi TK, Lee YB, et al. (2016a). A graphene-based electrochemical device with thermoresponsive microneedles for diabetes monitoring and therapy. *Nat Nanotechnol* 11:566–72.
- Lee H, Lee JH, Kim J, et al. (2016b). Hyaluronate-gold nanorod/DR5 antibody complex for noninvasive theranosis of skin cancer. *ACS Appl Mater Interfaces* 8:32202–10.
- Li Z, Chen Y, Yang Y, et al. (2019). Recent advances in nanomaterials-based chemo-photothermal combination therapy for improving cancer treatment. *Front Bioeng Biotechnol* 7:293.
- Matai I, Kaur G, Soni S, et al. (2020). Near-infrared stimulated hydrogel patch for photothermal therapeutics and thermoresponsive drug delivery. *J Photochem Photobiol B* 210:111960.
- Menon GK, Cleary GW, Lane ME. (2012). The structure and function of the stratum corneum. *Int J Pharm* 435:3–9.
- Mulik R, Kulkarni V, Murthy RSR. (2009). Chitosan-based thermosensitive hydrogel containing liposomes for sustained delivery of cytarabine. *Drug Dev Ind Pharm* 35:49–56.
- Murthy SN, Sammeta SM, Bowers C. (2010). Magnetophoresis for enhancing transdermal drug delivery: mechanistic studies and patch design. *J Control Release* 148:197–203.
- Neubert RH. (2011). Potentials of new nanocarriers for dermal and transdermal drug delivery. *Eur J Pharm Biopharm* 77:1–2.
- Pitorre M, Gondé H, Haury C, et al. (2017). Recent advances in nanocarrier-loaded gels: which drug delivery technologies against which diseases? *J Control Release* 266:140–55.
- Prausnitz MR. (1999). A practical assessment of transdermal drug delivery by skin electroporation. *Adv Drug Deliv Rev* 35:61–76.
- Prausnitz MR. (2004). Microneedles for transdermal drug delivery. *Adv Drug Deliv Rev* 56:581–7.
- Rai VK, Mishra N, Yadav KS, et al. (2018). Nanoemulsion as pharmaceutical carrier for dermal and transdermal drug delivery: formulation development, stability issues, basic considerations and applications. *J Control Release* 270:203–25.
- Roberts MS, Mohammed Y, Pastore MN, et al. (2017). Topical and cutaneous delivery using nanosystems. *J Control Release* 247:86–105.

- Schmolka IR. (1972). Artificial skin. I. Preparation and properties of pluronic F-127 gels for treatment of burns. *J Biomed Mater Res* 6:571–82.
- Seong JS, Yun ME, Park SN. (2018). Surfactant-stable and pH-sensitive liposomes coated with N-succinyl-chitosan and chitoooligosaccharide for delivery of quercetin. *Carbohydr Polym* 181:659–67.
- Siu KS, Chen D, Zheng X, et al. (2014). Non-covalently functionalized single-walled carbon nanotube for topical siRNA delivery into melanoma. *Biomaterials* 35:3435–42.
- Soga O, van Nostrum C, Fens M, et al. (2005). Thermosensitive and biodegradable polymeric micelles for paclitaxel delivery. *J Control Release* 103:341–53.
- Su G, Miao D, Yu Y, et al. (2019). Mesoporous silica-coated gold nanostars with drug payload for combined chemo-photothermal cancer therapy. *J Drug Target* 27:201–10.
- Wang Y, Thakur R, Fan Q, et al. (2005). Transdermal iontophoresis: combination strategies to improve transdermal iontophoretic drug delivery. *Eur J Pharm Biopharm* 60:179–91.
- Wichterle O, Lim D. (1960). Hydrophilic gels for biological use. *Nature* 185:117–8.
- Wu P, Yin S, Liu T, et al. (2021). "Building-block crosslinking" micelles for enhancing cellular transfection of biocompatible polycations. *Sci China Mater* 64:241–51.
- Yang Y, Pearson RM, Lee O, et al. (2014). Dendron-based micelles for topical delivery of endoxifen: a potential chemo-preventive medicine for breast cancer. *Adv Funct Mater* 24:2442–9.
- Yu Y, Zhou M, Zhang W, et al. (2019). Rattle-type gold nanorods/porous-SiO₂ nanocomposites as near-infrared light-activated drug delivery systems for cancer combined chemo-photothermal therapy. *Mol Pharm* 16:1929–38.
- Yue C, Liu P, Zheng M, et al. (2013). IR-780 dye loaded tumor targeting theranostic nanoparticles for NIR imaging and photothermal therapy. *Biomaterials* 34:6853–61.
- Zhang C, Liu T, Su Y, et al. (2010). A near-infrared fluorescent heptamethine indocyanine dye with preferential tumor accumulation for in vivo imaging. *Biomaterials* 31:6612–7.
- Zhang E, Luo S, Tan X, Shi C. (2014). Mechanistic study of IR-780 dye as a potential tumor targeting and drug delivery agent. *Biomaterials* 35:771–8.